Journal of Solution Chemistry, Vol. 34, No. 5, May 2005 (© 2005)
DOI: 10.1007/s10953-005-5590-y

Solvation Phenomena of Potassium Thiocyanate in Methanol–Water Mixtures

Abdul Wahab[1] **and Sekh Mahiuddin**[1,*]

Received July 7, 2004; revised December 16, 2004

This paper reports the results of a variety of experiments carried out for understanding the solvation behavior of potassium thiocyanate in methanol–water mixtures. Electrical conductivity, speed of sound, viscosity, and FT-Raman spectra of potassium thiocyanate solutions in 5 and 10% methanol–water (w/w) mixtures were measured as functions of concentration and temperature. The conductivity and structural relaxation time suggest the ion–solvent and solvent-separated ion–ion associations increase as the salt concentration increases in the mixtures. The Raman band shifts due to the C—O stretching mode of methanol for the solvent mixtures reveal the formation of methanol–water complexes. The significant changes in the Raman bands for the C—N, C—S and O—H stretching modes indicate the presence of SCN^-—solvent interactions through the N-end, "free" SCN^- and the solvent-shared ion pairs as potassium thiocyanate is added to the methanol–water mixtures. The relative changes corresponding to H—O—H bending and C—O stretching frequencies indicate that K^+ is preferentially solvated by water in these solvent mixtures. The appearance and increase of the intensity of a broad band at $\approx$940 cm^{-1} upon salt addition was attributed to the SCN^-–H_2O—K^+ solvent-shared ion pairs. No Raman spectral evidence for $K^+(H_2O)_n$ species was observed. The preferential solvation of K^+ and SCN^- in the methanol—water mixtures was verified by the application of the Kirkwood—Buff theory of solutions. This theory confirms that K^+ is strongly preferentially solvated by water, whereas SCN^- is preferentially solvated by the methanol component.

KEY WORDS: Electrical conductivity; methanol–water mixture; potassium thiocyanate; Raman spectra; solvation; structural relaxation time.

1. INTRODUCTION

The study of the solvation, particularly the preferential solvation phenomena of ions in mixed solvents, has attracted much attention in recent times because of its theoretical and practical importance.[1–4] Among the nonaqueous solvents,

[1]Material Science Division, Regional Research Laboratory, Jorhat-785 006, Assam, India; e-mail: mahirrljt@yahoo.com.

methanol is interesting because of the presence of both hydrophobic and hydrophilic groups and extensive H-bonding.

Methanol–water mixtures have excellent solvent properties[5] and are widely used as mobile phases in liquid chromatography. From the measurements of the volume change upon mixing, refractive index and density, Katz *et al.*[6,7] concluded that methanol–water mixtures form a ternary system and consist of clusters of methanol, water and methanol–water complexes. Pálinkás *et al.*[8] reported heat capacities of methanol–water mixtures and observed a maximum heat capacity at a low methanol mole fraction ($X_M = 0.116$). Takamuku *et al.*[9] made a detailed investigation of methanol–water mixtures using mass spectrometry and X-ray diffraction, and proposed that tetrahedral-like water clusters exist predominantly at $0 < X_M < 0.3$ and beyond $X_M = 0.3$ chain-like methanol clusters evolve. Zhao and Malinowski[5] measured the IR spectra of methanol–water mixtures in the complete composition range in the 1850–2700 cm^{-1} range and suggested that a complex consisting of two water molecules and one methanol molecule is formed. From the study of excess thermodynamic properties, Koga and coworkers[10,11] concluded that methanol molecules enhance the H-bonding network of water in their immediate vicinity in the water-rich region of methanol–water mixtures.

Physicochemical properties like the electrical conductivity of aqueous[12] and methanolic[13,14] solutions, the isentropic compressibility of aqueous and methanolic[15] solutions, the viscosity of aqueous[15,16] and methanolic[13,15] solutions, and the mutual diffusion coefficients and osmotic coefficients of aqueous[16] potassium thiocyanate solutions have been reported. However, such studies for potassium thiocyanate in mixed aqueous solvents are scarce.

The C—N (ν_3) and C—S (ν_1) stretching modes of SCN^- that appear at around 2060 and 750 cm^{-1}, respectively, and the water libration region, are very sensitive to electrostatic interactions and shift their peak frequencies accordingly.[17–20] Significant changes of these bands (ν_3 and ν_1) have led to a number of spectroscopic investigations[19,21–24] towards understanding the ion–solvent and ion–ion interactions in thiocyanate solutions. If a metal ion in aqueous solution forms a stable configuration like $[M^{m+}(H_2O)_n]$, there will be a symmetric stretching Raman band in the low frequency region due to water libration (ν_{lib}). The ν_{lib} bands for hydrated Li^+ and Na^+ species have been observed at $\approx$255 and $\approx$180 cm^{-1}, respectively.[17,18,20] Raman spectra of methanol–water mixtures[25,26] and that of the potassium thiocyanate in water[27–29] have been studied, but no report of a Raman spectroscopic investigation of potassium thiocyanate in methanol–water mixtures was found in the literature.

The Kirkwood–Buff theory[30] is one of the most valuable theories of solutions and is essentially a statistical–mechanical approach, which directly correlates the thermodynamic quantities with the solution structure without any assumptions.

The theory is based on the Kirkwood–Buff integrals:

$$G_{i\alpha} = \int_0^\infty 4\pi r^2 [g_{i\alpha}(r) - 1]\, dr \tag{1}$$

where $g_{i\alpha}(r)$ is the pair-correlation function for solvent α around solute particle i and r is the distance of α from the centre of i. The Kirkwood–Buff integrals, $G_{i\alpha}$, may be determined from the experimental data of such thermodynamic quantities as chemical potential, partial molar volume and isothermal compressibility in the light of the Ben-Naim[31] and Newman[32] approaches. Exploiting the idea extended by Ben-Naim[31] and others,[32,33] the preferential solvation parameter, $\delta X_{i\alpha}$ (*i.e.*, the local excess or deficit of each solvent near the solute relative to the bulk composition in a very dilute solution of solute i) can be estimated.

Therefore, in this paper the electrical conductivity, speed of sound, viscosity and FT-Raman spectra of potassium thiocyanate solutions in 5 and 10% methanol–water (w/w) mixtures, respectively, are reported as functions of salt concentration and temperature to sort out the different kinds of interactions and species present in the solutions. Finally, the Kirkwood–Buff theory[30] is used to verify the preferential solvation behavior of K^+ and SCN^- in methanol–water mixtures.

2. EXPERIMENTAL

Potassium thiocyanate (>97%, Qualigens Fine Chemicals, India) was recrystallized twice from double-distilled water and dried in a vacuum desiccator over P_2O_5. Anhydrous methanol was prepared from A. R. grade methanol (>99.5%, Qualigens Fine Chemicals, India) as described elsewhere.[34] All the solutions were prepared by mass with an accuracy of ±0.2% except for very dilute solutions for conductivity measurements that were prepared volumetrically by successive dilution of a stock solution.

Electrical conductivity was measured using a precision component analyser 6440A (Wayne Kerr, UK) having four terminal connectors at 1 kHz and a cell having platinised platinum electrodes. The cell constant was determined by using a 0.1 mol-kg^{-1} aqueous KCl solution at different temperatures and the conductivities of some standard electrolyte solutions were also checked to ascertain the cell constant. The density was measured by using a pycnometer. The measurements of the speed of sound and viscosity were performed with an ultrasonic interferometer at 2 MHz and a Schott-Geräte AVS 310 unit, respectively, as described earlier.[15,24] The accuracies of the conductivity, density, speed of sound and viscosity measurements were within ±0.02, ±0.01 ±0.01 and ±0.4%, respectively.

FT-Raman spectra were recorded at room temperature with a Bruker IFS 66 V optical bench with a FRA 106 Raman module attached to it. The light was excited at 1064 nm using a Nd:YAG laser. Laser power was set at 200 mW and 250 averaged

scans were accumulated with a resolution of 2 cm^{-1}. The spectra were recorded at the Sophisticated Analytical Instrumentation Facility, Indian Institute of Technology, Madras, India. All the measurements were performed as functions of the salt concentration ($0.1239 \leq m/\text{mol-kg}^{-1} \leq 20.30$) in a 5% methanol–water mixture and ($0.1073 \leq m/\text{mol-kg}^{-1} \leq 20.14$) in a 10% methanol−water mixture at temperatures of ($273.15 \leq T/\text{K} \leq 323.15$). Conductivity was also measured at low salt concentrations ($0.0009 \leq C/\text{mol-dm}^{-3} \leq 0.0100$). A thermostat unit, Julabo F 32, was used to maintain the temperature of the solutions within ±0.02 K.

3. RESULTS AND DISCUSSION

3.1. Electrical Conductivity and Structural Relaxation Time

The experimental electrical conductivity, κ, density, ρ, speed of sound, u, and viscosity, η, data of potassium thiocyanate in 5 and 10% methanol–water mixtures are listed in Tables AI–AIV, (Appendix & Supplementary materials), respectively, as functions of concentration and temperature. The conductivity data of very dilute solutions (0.0009–0.0100) mol-dm^{-3} were analysed using the Fuoss-Hsia conductance equation[35] of the form:

$$\Lambda = \Lambda_o - S(C\alpha)^{1/2} + EC\alpha \ \log(C\alpha) + J_1 C\alpha + J_2(C\alpha)^{3/2} - K_A(C\alpha)\gamma_{\pm}^2\Lambda \tag{2}$$

where the symbols have their usual meaning. The significant feature of Eq. (2) is that it provides the limiting molar conductivity, Λ_o, the association constant, K_A, and the interionic distance parameter, $\mathring{a}$. The values of the parameters, Λ_o, K_A and $\mathring{a}$ along with the standard deviation, σ, at three temperatures are collected in Table I.

It is apparent from Table I that potassium thiocyanate exhibits little or weak association in both the 5 and 10% methanol–water mixtures. Nevertheless, the

Table I. Values of the Parameters of Eq. (2) at Various Temperatures

T (K)	Λ_o (S-cm^2-mol^{-1})	K_A (dm^3-mol^{-1})	$\mathring{a}$ (Å)	σ
	5% Methanol–water mixture			
293.15	129.9	17.5	0.83	2.1
298.15	139.8	11.1	0.93	1.5
303.15	151.6	7.9	1.1	1.2
	10% Methanol–water mixture			
293.15	112.5	9.8	1.0	1.3
298.15	123.0	6.1	1.2	1.0
303.15	135.4	4.9	1.4	0.9

Note. Equation (2) could not be analysed for other temperatures due to lack of dielectric constant data.

association constant in the methanol–water mixtures increases with decreasing temperature, though the dielectric constant of the medium increases at low temperatures. Moreover, the H-bonding of water is reinforced at low temperatures[36,37] and also low temperature favors the ion-pair (solvent-separated, solvent-shared or contact) formation.[38] This might suggest that low temperature facilitates ion association in the methanol–water mixtures. However, Barthel *et al.*[14] found a decreasing trend of the association constant with decreasing temperature for potassium thiocyanate in pure methanol and at 298.15 K where the value of K_A is 18.3 dm^3-mol^{-1}.

To derive structural information in different concentration regions, the structural relaxation time, τ, is calculated for all the solutions using the relation:

$$\tau = \frac{4}{3}\eta u^{-2}\rho^{-1} \tag{3}$$

The κ *versus m* and τ *versus m* isotherms of the potassium thiocyanate solutions at three temperatures are illustrated in Figs. 1 and 2 for both 5 and 10% methanol–water mixtures, respectively. From Fig. 1, it is evident that the κ *versus m* isotherms in both the solvent mixtures pass through a maximum at ~9.5 mol-kg^{-1}. The specific conductivity, κ, of potassium thiocyanate in both the solvent mixtures

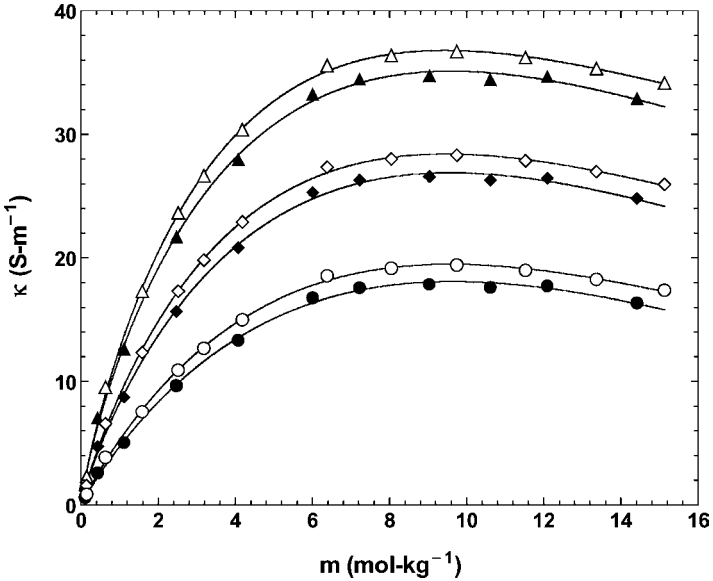

Fig. 1. Variation of electrical conductivity with molality at 273.15 K (◯, •), 298.15 K (◇, ◆), and 323.15 K (△, ▲) for potassium thiocyanate in 5 and 10% methanol–water mixtures. Open symbols and solid symbols represent 5 and 10% methanol–water mixtures, respectively.

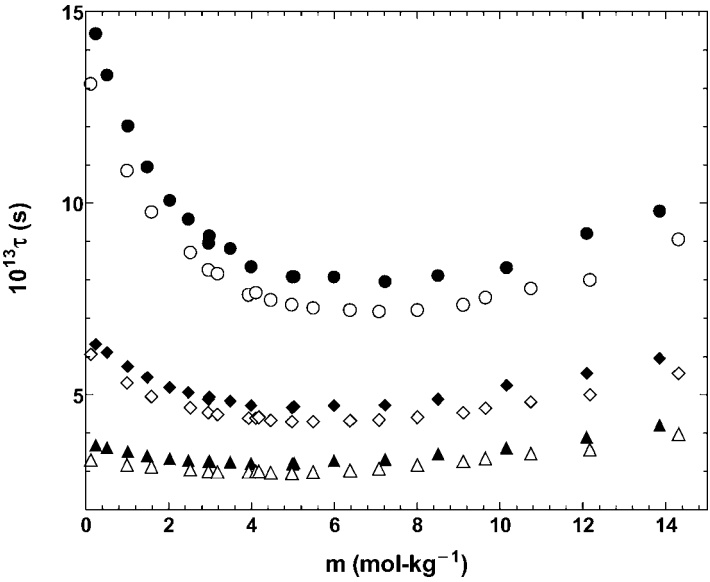

Fig. 2. Variation of structural relaxation time with molality at 273.15 K (◯, ●), 298.15 K (◇, ◆) and 323.15 K (△, ▲) for potassium thiocyanate in 5 and 10% methanol−water mixtures. Open symbols and solid symbols represent 5 and 10% methanol–water mixtures, respectively.

increases as the salt concentration increases up to around 9.5 mol-kg^{-1} and beyond 9.5 mol-kg^{-1} it decreases slowly. The presence of a conductivity maximum in the intermediate concentration region may be due to some kind of ionic association because of the decreasing number of available solvent molecules. This conclusion is consistent with other conductivity studies.[39] It should be noted here that a smaller number of solvent molecules are required to solvate associated ions than to solvate free ions. However, when the methanol content is increased in the solvent mixture by 5% (w/w), the conductivity shows a decreasing trend up to *ca.* 10% depending on the concentration and temperature of the solutions, suggesting slower solvation dynamics are induced by methanol addition.

Unlike the κ *versus* m plots, τ *versus* m isotherms in both 5 and 10% methanol–water mixtures decrease with the increase in concentration (Fig. 2). A similar variation was also observed for aqueous potassium thiocyanate solutions, but in methanolic solutions, the relaxation time increases with the increase in concentration.[15] From the decreasing trend in τ values at the early stages of salt addition in water or methanol–water mixtures, one can envisage the presence of a strongly bonded network structure of the solvent that is probably destabilised as the salt is added. It is apparent from Fig. 2 that the τ value decreases up to certain concentration and then increases slowly as the salt concentration increases. The

minimum in the τ *versus m* isotherms appears at ~7.0, ~6.0, and ~5.0 mol-kg^{-1} for 273.15, 298.15, and 323.15 K, respectively, in both the 5 and 10% methanol–water mixtures. The minimum at low temperatures is more pronounced than at higher temperatures.

The reinforced H-bonding at low temperatures[36,37] should contribute a higher τ value, whereas K^+ breaks the structure of the surrounding solvent. As a result, up to ~7.0 mol-kg^{-1} at low temperature (273.15 K), the resulting effect of the reinforced H-bonding among the solvent molecules and the structure breaking effect of K^+ causes a decrease in τ values with concentration and beyond ~7.0 mol-kg^{-1} ion-pair (solvent-separated and/or solvent-shared) formation causes increasing of τ values. However, at a higher temperature (323.15 K), thermal vibrations govern the relaxation processes over the above-mentioned controlling effects. In methanol, K^+ has no structure-breaking influence. Recently, Hawlicka and Swiatla-Wojcik[40] proposed the existence of ion pairs and multiple ion aggregates of sodium halides in methanol–water mixtures at moderate concentrations (1.1–0.55 mol-dm^{-3}) from molecular dynamics simulations. The overall behavior of conductivity and structural relaxation time suggests that below 8.0 mol-kg^{-1} either solvent–solvent or ion–solvent or both interactions are predominant, and beyond 8.0 mol-kg^{-1} ionic interactions come into play resulting in the formation of solvent-separated and/or solvent-shared ion pairs.

3.2. FT-Raman Spectra

To shed more light on the interactions and species present in the solutions under investigation, FT-Raman spectra were recorded as a function of salt concentration. The Raman spectra of potassium thiocyanate solutions in methanol–water mixtures at various salt concentrations are presented in Figs. 3–6 including the solvent mixture spectra. The band assignments and position of the principal bands are summarised in Table II. Band assignments of the solvent mixtures as well as the aqueous and methanolic thiocyanate solutions were made by several authors.[22,23,25–29,41]

3.2.1. The Water Libration Region

In the water libration region (Figs. 3 and 4) only three bands at around 85, 123 and 450 cm^{-1} are observed in the methanol–water mixtures and in potassium thiocyanate solutions. The two low-frequency bands at around 85 and 123 cm^{-1} with a shoulder at ≈170 cm^{-1} (marked by an arrow) in the present systems may originate from the O- -H–O bending and stretching vibrations of H-bonded water molecules in a tetrahedral water structure (restricted translatory mode).[18,41] In pure water the restricted translatory modes are observed in the 60–70 and 170–190 cm^{-1} ranges.[18,20,41] The contour of the shoulder (at ≈170 cm^{-1})

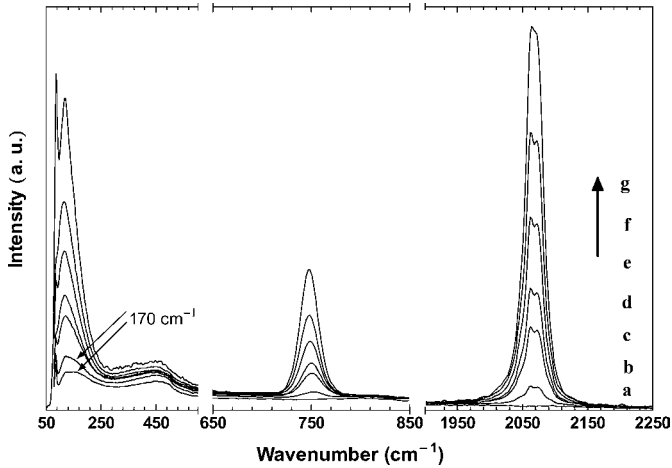

Fig. 3. The Raman spectra of (a) the solvent mixture, (b) 0.5775, (c) 2.411, (d) 4.035, (e) 7.990, (f) 11.11, and (g) 20.30 mol-kg^{-1} potassium thiocyanate in a 5% methanol–water mixture in the 50–850 and 1900–2250 cm^{-1} ranges.

vanishes as the salt concentration increases (>0.5775 and 1.101 mol-kg^{-1} in 5 and 10% methanol–water mixtures, respectively) and is, therefore, accounted for the O- -H–O stretching vibrations of the "free" water which is not involved in the methanol–water complexes. The formation of methanol–water complexes is an established fact in methanol–water mixtures.[5–7,9] The broad band due to the

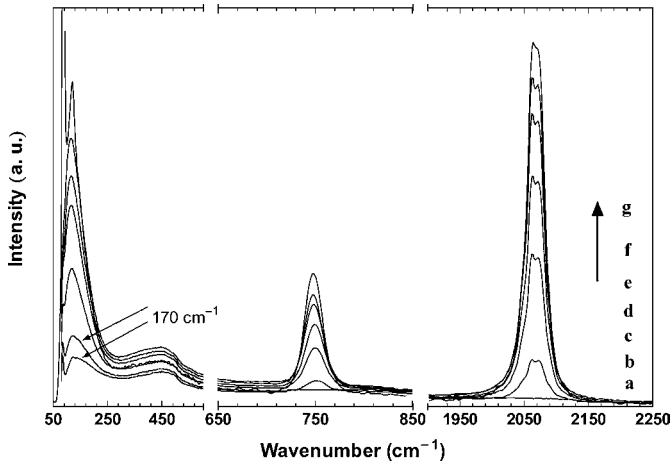

Fig. 4. The Raman spectra of (a) the solvent mixture, (b) 1.101, (c) 4.195, (d) 6.028, (e) 8.038, (f) 11.06, and (g) 20.14 mol-kg^{-1} potassium thiocyanate in 10% methanol–water mixture in the 50–850 and 1900–2250 cm^{-1} ranges.

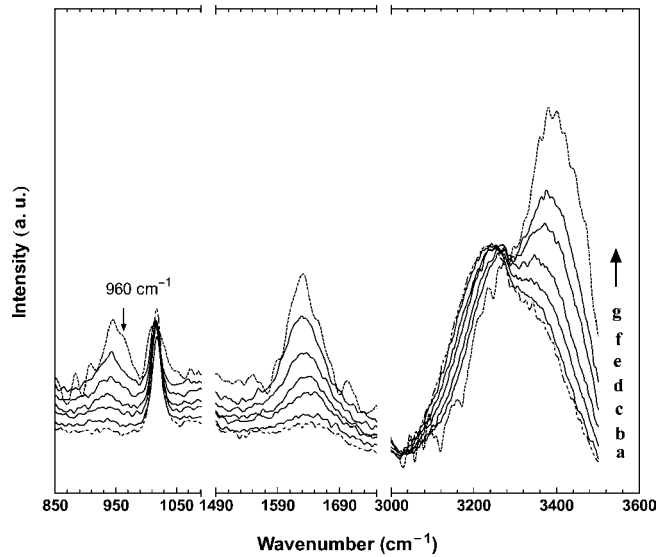

Fig. 5. The Raman spectra of (a) the solvent mixture, (b) 0.5775, (c) 2.411, (d) 4.035, (e) 7.990, (f) 11.11, and (g) 20.30 mol-kg^{-1} potassium thiocyanate in 5% methanol–water mixture in the 850–1090, 1490–1750, and 3020–3500 cm^{-1} ranges.

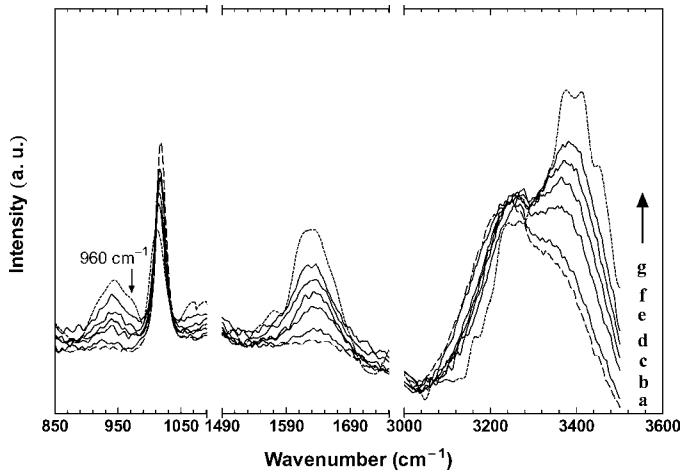

Fig. 6. The Raman spectra of (a) the solvent mixture, (b) 1.101, (c) 4.195, (d) 6.028, (e) 8.038, (f) 11.06, and (g) 20.14 mol-kg^{-1} potassium thiocyanate in 10% methanol–water mixture in the 850–1090, 1490–1750, and 3020–3500 cm^{-1} ranges.

Table II. Band Assignments and Positions (Wavenumbers) for Methanol–Water Mixtures and Their Potassium Thiocyanate Solutions

Assignments of modes	Band position (cm^{-1})						
	5% Methanol–water mixture						
	Solvent mixture	0.5775 ($mol\text{-}kg^{-1}$)	2.411 ($mol\text{-}kg^{-1}$)	4.035 ($mol\text{-}kg^{-1}$)	7.990 ($mol\text{-}kg^{-1}$)	11.11 ($mol\text{-}kg^{-1}$)	20.30 ($mol\text{-}kg^{-1}$)
O- -H−O bend	85 (*s*)	85 (*s*)	86 (*w*)		87 (*w*)		87 (*vs*)
O- -H−O stretch	123 (*b*)	122 (*m*)	121 (*m*)	119 (*s*)	118 (*s*)	116 (*s*)	118 (*s*)
	170 (*b*)	170 (*b*)	170 (*b*)				
Libration	454 (*b*)	453 (*b*)	452 (*b*)	451 (*b*)	445 (*b*)	434 (*b*)	442 (*b*)
C−S stretch		753 (*b*)	751 (*s*)	750 (*s*)	749 (*vs*)	749 (*vs*)	748 (*vs*)
$SCN^- - H_2O - K^+$			939 (*b*)	936 (*b*)	942 (*b*)	943 (*b*)	945 (*b*)
C−O stretch	1018 (*vs*)	1018 (*vs*)	1017 (*vs*)	1017 (*vs*)	1015 (*vs*)	1015 (*vs*)	1013 (*vs*)
H−O−H bend	1645 (*w*)	1643 (*b*)	1643 (*m*)	1639 (*s*)	1632 (*s*)	1628 (*s*)	1630 (*s*)
C−N stretch		2062 (*b*)	2062 (*vs*)	2062 (*vs*)	2062 (*vs*)	2062 (*vs*)	2062 (*vs*)
		2073 (*b*)	2072 (*vs*)	2072 (*vs*)	2071 (*vs*)	2071 (*vs*)	2069 (*vs*)
O−H stretch	3243 (*b*)	3252 (*b*)	3255 (*b*)	3262 (*b*)	3265 (*b*)	3275 (*b*)	3278 (*b*)
	3350 (*w*)	3355 (*w*)	3255 (*b*)	3356 (*b*)	3372 (*b*)	3378 (*b*)	3393 (*b*)
	10% Methanol−water mixture						
	Solvent mixture	1.101 ($mol\text{-}kg^{-1}$)	4.195 ($mol\text{-}kg^{-1}$)	6.028 ($mol\text{-}kg^{-1}$)	8.038 ($mol\text{-}kg^{-1}$)	11.06 ($mol\text{-}kg^{-1}$)	20.14 ($mol\text{-}kg^{-1}$)
O- -H−O bend	85 (*s*)	85 (*s*)	87 (*w*)	87 (*vw*)			87 (*vs*)
O- -H−O stretch	123 (*b*)	122 (*m*)	119 (*m*)	117 (*s*)	116 (*s*)	116 (*s*)	120 (*s*)
	170 (*b*)	170 (*b*)					
Libration	453 (*b*)	451 (*b*)	450 (*b*)	447 (*b*)	444 (*b*)	442 (*b*)	440 (*b*)
C−S stretch		751 (*b*)	750 (*s*)	749 (*s*)	748 (*vs*)	747 (*vs*)	747 (*vs*)
$SCN^- - H_2O - K^+$			940 (*b*)	939 (*b*)	940 (*b*)	940 (*b*)	944 (*b*)
C−O stretch	1018 (*vs*)	1018 (*vs*)	1017 (*vs*)	1017 (*vs*)	1016 (*vs*)	1015 (*vs*)	1013 (*vs*)
H−O−H bend	1637 (*w*)	1636 (*b*)	1631 (*m*)	1631 (*s*)	1630 (*s*)	1628 (*s*)	1627 (*b*)
C−N stretch		2062 (*s*)	2062 (*vs*)	2063 (*vs*)	2062 (*vs*)	2062 (*vs*)	2062 (*vs*)
		2073 (*s*)	2072 (*vs*)	2072 (*vs*)	2072 (*vs*)	2071 (*vs*)	2069 (*vs*)
O−H stretch	3242 (*b*)	3250 (*b*)	3261 (*b*)	3263 (*b*)	3270 (*b*)	3270 (*b*)	3270 (*b*)
	3350 (*w*)	3352 (*w*)	3356 (*b*)	3365 (*b*)	3372 (*b*)	3382 (*b*)	3395 (*b*)

Note. b, broad; m, medium; w, weak; vw, very weak; s, sharp; vs, very sharp.

libration of water molecules at ≈450 cm^{-1} in solvent mixtures exhibits a red shift as the salt concentration increases.

It is worth noting that no band corresponding to the ν_{lib} mode of the $K^+(H_2O)_n$ species could be detected in the present study as predicted earlier.[1] The absence of the band could be interpreted by considering the low charge density and polarising power of K^+. Consequently, no stable $K^+(H_2O)_n$ species are possible. From Raman spectral investigations of aqueous alkali thiocyanates, Kato *et al.*[27–29] inferred that as the size of the alkali cation increases, the aquation forces become weaker. Recently, QM/MM molecular dynamics simulations[42] on the hydrated water molecules of Na^+ and K^+ have indicated that K^+ has a weak influence on the water molecules in the hydration shell rather than perturb the surrounding solvent environment.

3.2.2. The C—N and C—S Stretching Region

The C—N stretching region shows two growing sharp peaks at 2062 and 2073 cm^{-1} as is shown in Figs. 3 and 4 for 5 and 10% methanol–water mixtures, respectively. The position of the peak at 2062 cm^{-1} is independent of the solvent composition as well as the salt concentration, but the peak at 2073 cm^{-1} shows a small red shift ($\Delta\nu \approx 4$ cm^{-1}) as the salt concentration increases in both the 5 and 10% methanol–water mixtures. In other words, the 2073 cm^{-1} peak shows a blue shift with increasing solvent concentration implying more H-bonding interactions. For solid potassium thiocyanate a single sharp band at ≈2050 cm^{-1} was observed.[43] In earlier studies,[19,21] it was proven that H-bonding along the molecular axis to either end of SCN^- leads to a positive frequency shift for the C—N mode. Accordingly, the band at 2062 cm^{-1} is attributed to "spectroscopically free" SCN^- and the band at 2073 cm^{-1} can be accounted for the N-end H-bonded OH—NCS^- species. The presence of "free" SCN^- species in methanolic solutions was proposed elsewhere from IR spectral investigations.[19,22] At the highest salt concentrations (∼20 mol-kg^{-1}), the peak at 2073 cm^{-1} is red shifted to 2069 cm^{-1}, which also implies weakening of the C≡N bond probably due to the non-axial H-bonding interactions with the π-electrons of SCN^-.[22]

The C—S stretching mode at around 752 cm^{-1} also exhibits a small red shift of ≈5 cm^{-1} as the salt concentration increases (Figs. 3 and 4). The red shift may be due to the presence of a small percentage of H-bonding through the S-end of SCN^- with solvent molecules at dilute concentrations. The extensive occurrence of hydrogen bonding of SCN^- through the N-end is reasonable because N-center is a better hydrogen bond acceptor than the S-center.[44] It is probable that as the salt concentration increases the OH—NCS^- bonded water molecules may also enter the primary solvation shell of the cation due to the decreasing number of solvent molecules (beyond 8.0 mol-kg^{-1}) leading to the formation of solvent-separated and/or solvent-shared ion pairs.

3.2.3. The C—O Stretching and H—O—H Bending Region

It is well established from X-ray and neutron diffraction studies[45] that cations often exhibit a definitive solvation shell because of their small size and strong ion–solvent interactions compared to anions. When the solvent is water or methanol, the cation–solvent interactions are dominated by electrostatic interactions through the solvent oxygen atom, whereas anion–solvent interactions are primarily due to H-bonding with the hydrogen atom approaching the ion.[45,46] Such cation–solvent interactions should influence the band frequency of H—O—H bending or C—O stretching of methanol. Thus, preferential solvation in methanol–water mixtures could be evidenced from the relative spectral changes corresponding to the H—O—H bending and C—O stretching modes of methanol.

The C—O stretching mode for pure methanol appears at 1035 cm^{-1}.[25] The present solvent mixtures show a sharp band at around 1018 cm^{-1} corresponding to the C–O stretching mode of methanol resulting from a shift of $\Delta\nu \approx 17$ cm^{-1} (Figs. 5 and 6). A similar observation of band shifting was reported.[25,26] Such large red shifts for the C—O mode in the mixtures are expected due to the involvement of the oxygen atom of methanol as a H-bond acceptor in the methanol–water complexes. The band due to C—O stretching exhibits a small red shift ($\Delta\nu \approx 4$ cm^{-1}) with decreasing intensity as the salt concentration is increased in the mixtures. On the other hand, a broad band for the H—O—H bending mode of water in the solvent mixtures appears near 1640 cm^{-1}. The band exhibits a large red shift ($\Delta\nu \approx 15$ cm^{-1} for the 5% methanol–water and $\Delta\nu \approx 10$ cm^{-1} for 10% methanol–water mixtures) with increased intensity as the salt concentration increases and is attributed to the hydration of the cation. Therefore, the observed frequency shift and intensity of the H—O—H bending mode compared to that of the C—O stretching mode of methanol favors the conclusion that water is preferentially solvated to K^+. Based on the Gibbs energy of transfer data from water to methanol–water mixtures, Wells[47] suggested a weak preferential solvation of alkali metal ions by water in the water-rich region, but in the methanol-rich region a preferential solvation by methanol was argued.

In the more concentrated solutions ($\geq$4.035 and 4.195 mol-kg^{-1} in 5 and 10% methanol–water mixtures, respectively), a broad band at $\approx$940 cm^{-1} appears for both the 5 and 10% methanol—water mixtures (Figs. 5 and 6). The band exhibits a blue shift ($\Delta\nu \approx 5$ cm^{-1}) with growing intensity as the salt concentration increases. The band is attributed to SCN^-–H_2O–K^+ solvent-shared ion pairs. A similar type of solvent-shared ion pair was reported corresponding to a band at $\approx$931 cm^{-1} in the IR spectra of Li, Na and Mg perchlorate solutions in propylene carbonate–water mixtures.[39] In the highest concentrations (20.30 and 20.14 mol-kg^{-1} in Figs. 5 and 6, respectively), a shoulder at $\approx$960 cm^{-1} appeared (marked by an arrow) at the high frequency side with respect to the $\approx$940 cm^{-1} band and can be assigned to the occurrence of contact ion pairs.

3.2.4. The O—H Stretching Region

It is apparent from the Figs. 5 and 6 that the O—H stretching region (3100–3500 cm^{-1}) shows some striking features in the spectra of solvent mixtures as well as potassium thiocyanate solutions. Both the aqueous and methanolic O—H stretching modes superimpose in this region. Several studies[25,48–50] concluded that intermolecular hydrogen bonding is responsible for the extreme broad nature of the O—H stretching band and anions strongly influence this band. For the solvent mixtures an intense broad band centered at ≈3243 cm^{-1} with a weak shoulder at ≈3350 cm^{-1} is observed. However, upon addition of potassium thiocyanate, the band at 3350 cm^{-1} grows in intensity and shifts to a higher frequency region. For ∼20 mol-kg^{-1}, the band at 3350 cm^{-1} is shifted to ≈3393 cm^{-1} (Figs. 5 and 6). On the other hand, the intensity of the 3243 cm^{-1} band remains almost constant, but shifts to a higher frequency region with increasing salt concentration. The intensities of the bands at 3243 and 3350 cm^{-1} become nearly equal at 7.990 and 6.028 mol-kg^{-1} solutions in the 5 and 10% methanol—water mixtures, respectively.

The band at ≈3243 cm^{-1} is assigned to the O—H stretching mode, which is involved in the methanol–water mixed complexes. The broad band at ≈3350 cm^{-1} is ascribed to the O—H stretching mode arising from the OH groups directly hydrogen bonded to SCN^- and also from the coordination of K^+ by forming solvent-shared ion pairs at higher salt concentrations (>8.0 mol-kg^{-1}). In a previous Raman investigation, Rohman *et al.*[24] have suggested the formation of solvent-shared and contact ion pairs in aqueous and methanolic sodium thiocyanate solutions. Considering the trend of the positive frequency shift and intensities of the 940 and 3350 cm^{-1} bands in conjunction with the transport and relaxation behavior of the solutions, it can be concluded that the solvent structure is substantially disrupted beyond *ca.* 8.0 mol-kg^{-1} with the formation of solvent-separated and/or solvent-shared ion pairs in the solvent mixtures.

3.3. The Kirkwood–Buff Theory

The Kirkwood–Buff functions for both the K^+ and SCN^- in methanol–water mixtures were calculated using data from different sources[1,33,51–53] and are summarised in Table III. The required Gibbs energy of transfer, $\Delta_t G_i^o$, values for the ions from water to methanol–water mixtures were taken from the literature.[51,52] However, the Gibbs energies of transfer for SCN^- are available only up to $\sim X_M = 0.3$.[52] The data for isothermal compressibility, κ_T, molar volume, V, and excess molar Gibbs energy of mixing, G^E_{MW}, of the solvent mixtures were derived from literature values.[1,53] The partial molar volumes of the ions at infinite dilution and ionic sizes were obtained from Marcus's compilation[1] to calculate the correlation volumes, V_{cor}. Next, the excess or deficiency of water

Table III. The Kirkwood−Buff Parameters for the System KSCN in Methanol–Water Mixtures at 298.15 K

X_M	κ_T (GPa^{-1})[a]	$d^2G^E_{MW}/dX^2_M$ (kJ-mol^{-1})[b]	V (cm^3-mol^{-1})	$d\Delta_t G^o_i/dX_M$ (kJ-mol^{-1})[c]	V_{cor} (cm^3-mol^{-1})[d]	δX_{iW}
			K^+-Methanol–water system			
0.02	4.512	−5.89	18.46	24.08	171.6	0.022
0.05	4.436	−5.42	19.03	21.42	176.3	0.053
0.10	4.425	−4.69	19.98	17.69	184.1	0.094
0.15	4.497	−4.05	20.97	14.75	192.0	0.119
0.20	4.655	−3.48	21.96	12.50	200.2	0.130
0.25	4.861	−2.99	22.98	10.85	208.4	0.133
0.30	5.137	−2.58	24.02	9.701	216.8	0.132
0.35	5.457	−2.25	25.08	8.956	225.3	0.129
0.40	5.826	−2.00	26.16	8.520	233.9	0.128
0.45	6.224	−1.83	27.25	8.297	242.7	0.126
0.50	6.665	−1.74	28.37	8.190	251.5	0.125
0.55	7.146	−1.73	29.51	8.104	260.6	0.121
0.60	7.642	−1.79	30.67	7.942	269.7	0.115
0.65	8.195	−1.94	31.85	7.608	279.2	0.104
0.70	8.733	−2.17	33.05	7.006	288.5	0.088
0.75	9.325	−2.47	34.28	6.039	298.3	0.067
0.80	9.918	−2.85	35.53	4.613	308.0	0.043
0.85	10.54	−3.32	36.79	2.630	317.8	0.019
0.90	11.19	−3.86	38.09	−0.006	328.0	−0.00003
0.95	11.83	−4.48	39.40	−3.391	338.2	−0.0082
			SCN^--Methanol–water system			
0.02				−8.32	262.3	−0.006
0.05				−6.73	268.5	−0.012
0.10				−4.59	278.8	−0.017
0.15				−3.00	289.3	−0.016
0.20				−1.87	299.9	−0.013
0.25				−1.09	310.7	−0.009
0.30				−0.56	321.7	−0.005
0.35				−0.17	332.7	−0.002

[a] [53].
[b] [1], p. 190.
[c] [51] and [52].
[d] Ionic radii of K^+ and SCN^- were taken as 0.133 and 0.195 nm, respectively.

molecules in the vicinity of the ions, δX_{iW}, was estimated *via* the local mole fraction, X^L_{iW}, around the ion i:

$$\delta X_{iW} = X^L_{iW} - X_W \tag{4}$$

where X_W is the mole fraction of the bulk water. The estimated preferential solvation parameters for potassium thiocyanate and its ions are presented in Fig. 7 as a function of methanol mole fraction, X_M.

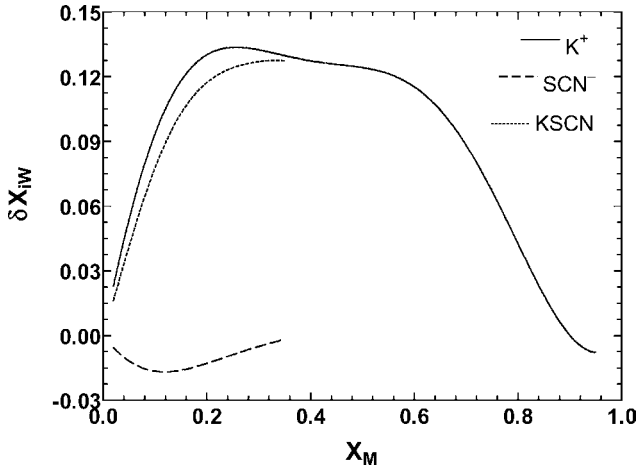

Fig. 7. Plots of the preferential solvation parameter for potassium thiocyanate and its ions in methanol–water mixtures at 298.15 K as a function of the methanol mole fraction.

The present systems falls within $X_M = 0.1$ and the results obtained from the calculations of the Kirkwood–Buff integrals (Fig. 7) can be summarised as follows. In the methanol–water mixtures, K^+ is strongly preferentially solvated by water up to $X_M =\sim 0.9$, beyond that methanol is preferred. Whereas SCN^- is preferentially solvated by methanol in the mixture up to $X_M =\sim 0.4$. The sum of the δX_{iW} values for both ions suggests overall selective solvation of KSCN by the water component in methanol–water mixtures. Thus, the preferential solvation of K^+ with water molecules is confirmed as was indicated by the Raman spectra. From the Kirkwood–Buff approach, Marcus[33] observed that the ions of NaCl and CsI are preferably solvated by water in methanol–water mixtures.

It is most interesting that SCN^- prefers methanol to water despite the fact that water is smaller and can produce maximum H-bonding. The preference of one solvent over the other seems to originate from two complementary factors: the orientation of solvent molecules in the electric fields of the ions and the tendency to preserve the H-bond connectivity of solvent molecules.[40] Smaller water molecules can easily orient in the field of K^+, whereas linear H-bonding between the SCN^- and solvent molecules might prefer methanol since SCN^- is known to act as a H-bond connector.[54]

4. CONCLUSIONS

Electrical conductivity, speed of sound, viscosity, and FT-Raman spectra of potassium thiocyanate in 5 and 10% methanol–water mixtures were measured as functions of concentration and temperature. Electrical conductivity, speed of

sound and viscosity results suggest that below 8.0 mol-kg^{-1} either solvent–solvent or ion–solvent or both interactions are predominant. Beyond 8.0 mol-kg^{-1} ion–ion interactions come into play resulting in solvent-separated and/or solvent-shared ion pairs increase owing to a decreasing number of available solvent molecules. The structure-breaking property of K^+ strongly influences the solution transport properties.

The Raman band shifts due to the C—O stretching mode of methanol in the solvent mixtures reveal the formation of strongly associated methanol–water complexes. On the other hand, the presence of a N-end SCN^-–solvent complex, "free" SCN^- species and solvent-shared ion pairs (SCN^-–H_2O—K^+) in the methanol–water mixtures are observed from the significant changes corresponding to the C—N, C—S and O—H stretching modes, upon salt addition. No Raman spectral evidence is found for the existence of $K^+(H_2O)_n$ cluster species. The relative shift of band parameters corresponding to the H—O—H bending and C—O stretching modes of methanol implies preferential solvation of K^+ by water molecules in the mixtures. The solvent structure is substantially disrupted beyond *ca*. 8.0 mol-kg^{-1} by the emergence of SCN^-–H_2O—K^+ species in the solution. Finally, the Kirkwood–Buff theory of solution was used to confirm the preferential solvation phenomena of the ions. The K^+ is strongly preferentially solvated by water, whereas SCN^- is preferentially solvated by the methanol component in the solvent mixtures.

ACKNOWLEDGMENTS

The authors are thankful to the director of the laboratory for the facilities and interest in this work. AW is grateful to the Council of Scientific & Industrial Research, New Delhi, for the award of a senior research fellowship. The authors are also thankful to the anonymous reviewers of this manuscript for valuable suggestions. The authors are also grateful to the Sophisticated Analytical Instrumentation Facility, Indian Institute of Technology-Madras, India for recording the raman spectra.

REFERENCES

1. Y. Marcus, *Ion Solvation* (Wiley, Chichester, UK, chapters 6, 7 and 9, 1985).
2. H.-J. Gores and J. Barthel, *Pure Appl. Chem.* **67**, 919 (1995).
3. H. Ohtaki, *Monatsh. Chem.* **132**, 1237 (2001).
4. A. Tongraar, K. Sagarik, and B. M. Rode, *Phys. Chem. Chem. Phys.* **4**, 628 (2002).
5. Z. Zhao and E. R. Malinowski, *Anal. Chem.* **71**, 602 (1999).
6. E. D. Katz, K. Ogan, and R. P. W. Scott, *J. Chromatogr.* **352**, 67 (1986).
7. E. D. Katz, C. H. Lochmuller, and R. P. Scott, *Anal. Chem.* **61**, 349 (1989).
8. G. Pálinkás, E. Hawlicka, and K. Heinzinger, *Chem. Phys.* **158**, 65 (1991).
9. T. Takamuku, T. Yamaguchi, M. Asato, M. Matsumoto, and N. Nishi, *Z. Naturforsch.* **55**a, 513 (2000).

10. S. H. Tanaka, H. I. Yoshihara, A. W. Ho, F. W. Lau, P. Westh, and Y. Koga, *Can. J. Chem.* **74**, 713 (1996).
11. J. Hu, C. A. Haynes, A. H. Y. Wu, C. M. W. Cheung, M. M. Chen, E. G. M. Yee, T. Ichioka, K. Nishikawa, P. Westh, and Y. Koga, *Can. J. Chem.* **81**, 141 (2003).
12. C. S. Pak and I. N. Maksimova, *Zh. Prikl. Khim.* (*Leningrad*) **58**, 491 (1985).
13. P. G. Sears and L. R. Dawson, *J. Chem. Eng. Data* **13**, 124 (1968).
14. J. Barthel, M. Krell, L. Iberl, and F. Feuerlein, *J. Electroanal. Chem.* **214**, 485 (1986).
15. N. Rohman, N. N. Dass, and S. Mahiuddin, *Aust. J. Chem.* **53**, 463 (2000).
16. J. P. Mitchell, J. B. Butler, and J. G. Albright, *J. Solution Chem.* **21**, 1115 (1992).
17. K. H. Michaelian and M. Moskovits, *Nature* **273**, 135 (1978).
18. W. Rudolph, M. H. Brooker, and C. C. Pye, *J. Phys. Chem.* **99**, 3793 (1995).
19. P. W. Schultz, G. E. Leroi, and A. I. Popov, *J. Am. Chem. Soc.* **118**, 10617 (1996).
20. Y. Kameda, K. Sugawara, T. Usuki, and O. Uemura, *Bull. Chem. Soc. Jpn.* **71**, 2769 (1998).
21. M. Chabanel, *Pure Appl. Chem.* **62**, 35 (1990).
22. M. Bachelin, P. Gans, and J. B. Gill, *J. Chem. Soc., Faraday Trans.* **88**, 3327 (1992).
23. J. B. Gill, in *Chemistry of Nonaqueous Solutions: Current Progress*, G. Mamantov and A. I. Popov, eds. (VCH Publishers, New York, chapter 2, 1994).
24. N. Rohman, A. Wahab, N. N. Dass, and S. Mahiuddin, *Fluid Phase Equilb.* **178**, 277 (2001).
25. R. E. Hester and R. A. Plane, *Spectrochim. Acta* **23**, 2289 (1967).
26. G. Kabisch and K. Pollmer, *J. Mol. Struct.* **81**, 35 (1982).
27. T. Kato and T. Takenaka, *Mol. Phys.* **46**, 257 (1982).
28. T. Kato, *Mol. Phys.* **48**, 1119 (1983).
29. T. Kato, *J. Chem. Phys.* **79**, 2139 (1983).
30. J. G. Kirkwood and F. P. Buff, *J. Chem. Phys.* **19**, 774 (1951).
31. A. Ben-Naim, *Cell Biophys.* **12**, 255 (1988).
32. K. E. Newman, *J. Chem. Soc., Faraday Trans. 1* **84**, 1387 (1988).
33. Y. Marcus, *J. Chem. Soc., Faraday Trans. 1* **85**, 3019 (1989).
34. A. I. Vogel, *A Textbook of Practical Organic Chemistry*, 3rd edn. (ELBS, Longman, UK, 1975), p. 268.
35. R. M. Fuoss and K. L. Hsia, *Proc. Natl. Acad. Sci. USA* **58**, 1808 (1967).
36. H. Hase, K. Ishioka, Y. Miyatake, M. Kabayashi, and M. Kabayashi, *J. Phys. Chem.* **95**, 8541 (1991).
37. K. Yamanaka, M. Yamagami, T. Takamuku, T. Yamaguchi, and H. Wakita, *J. Phys. Chem.* **97**, 10835 (1993).
38. P. Smirnov, M. Yamagami, H. Wakita, and T. Yamaguchi, *J. Mol. Liq.* **73**, 305 (1997).
39. N. D. Cvjetićanin and S. Mentus, *Phys. Chem. Chem. Phys.* **1**, 5157 (1999).
40. E. Hawlicka and D. Swiatla-Wojcik, *J. Chem. Phys.* **119**, 2206 (2003).
41. Y. Wang and Y. Tominaga, *J. Chem. Phys.* **101**, 3453 (1994).
42. A. Tongraar and B. M. Rode, *Chem. Phys. Lett.* **385**, 378 (2004).
43. I. A. Degen and G. A. Newman, *Spectrochim. Acta* **49**, 859 (1993).
44. S. Wojtulewski and S. J. Grabowski, *Chem. Phys. Lett.* **378**, 388 (2003).
45. H. Ohtaki and T. Radnai, *Chem. Rev.* **93**, 1157 (1993).
46. O. N. Kalugin and A. K. Adya, *Phys. Chem. Chem. Phys.* **2**, 11 (2000).
47. C. F. Wells, *J. Chem. Soc., Faraday Trans.* **69**, 984 (1973).
48. W. R. Busing and D. F. Hornig, *J. Phys. Chem.* **65**, 284 (1961).
49. H. Kanno and H. Hiraishi, *J. Phys. Chem.* **87**, 3664 (1983).
50. N. A. Chumaevskii, M. N. Rodnikova, and D. A. Sirotkin, *J. Mol. Liq.* **91**, 81 (2001).
51. C. Kalidas, G. Hefter, and Y. Marcus, *Chem. Rev.* **100**, 819 (2000).
52. C. Patra and P. K. Das, *Thermochim. Acta* **53**, 357 (1982).
53. G. Douheret and A. Khadir, *Thermochim. Acta* **142**, 219 (1989).
54. Y. Koga, P. Westh, J. V. Davies, K. Miki, K. Nishikawa, and H. Katayanagi, *J. Phys. Chem. A* **108**, 8533 (2004).

A1. APPENDIX

A1.1 Supplementary Materials

Table AI. Electrical Conductivity of Potassium Thiocyanate in Methanol−Water Mixtures as Functions of Salt Concentration and Temperature

T (K)	Λ (S-cm^2-mol^{-1})						
	5% Methanol−water mixture						
	0.00102 (*C*)	0.0016 (*C*)	0.0024 (*C*)	0.0032 (*C*)	0.0040 (*C*)	0.0052 (*C*)	0.0060 (*C*)
273.15	94.47	87.25	81.83	77.03	74.01	70.27	69.45
283.15	112.1	106.4	101.9	97.94	95.45	92.36	91.40
293.15	128.9	124.7	121.5	119.0	116.7	114.8	113.8
298.15	138.0	135.0	132.5	130.4	128.6	126.8	125.8
303.15	149.1	146.9	144.7	143.0	141.4	139.5	138.3
313.15	174.4	173.0	171.0	169.3	167.7	165.6	164.7
	0.0068 (*C*)	0.0080 (*C*)	0.0096 (*C*)				
273.15	68.76	68.63	68.51				
283.15	90.69	90.39	90.36				
293.15	113.2	113.1	112.8				
298.15	125.3	125.0	124.8				
303.15	138.0	137.6	137.5				
313.15	164.0	163.7	163.3				
	10% Methanol−water mixture						
	0.0009 (*C*)	0.0020 (*C*)	0.0032 (*C*)	0.0044 (*C*)	0.0056 (*C*)	0.0068 (*C*)	0.0090 (*C*)
273.15	78.18	67.50	63.16	61.51	60.55	59.75	58.79
283.15	97.00	87.35	83.81	82.30	81.25	80.47	79.03
293.15	112.0	107.2	104.6	103.4	102.4	101.5	100.6
298.15	122.0	118.0	115.9	114.8	113.8	113.0	112.3
303.15	134.0	130.2	127.9	126.8	125.7	125.1	124.1
313.15	160.1	155.8	153.6	151.9	151.0	150.1	149.2
	0.0100 (*C*)						
273.15	58.33						
283.15	78.17						
293.15	100.3						
298.15	111.9						
303.15	123.9						
313.15	148.8						
T (K)	κ (S-m^{-1})						
	5% Methanol−water mixture						
	0.1495 (*m*)	0.6352 (*m*)	1.589 (*m*)	2.524 (*m*)	3.184 (*m*)	4.183 (*m*)	6.382 (*m*)
273.15	0.8703	3.854	7.561	10.92	12.69	15.01	18.55
278.15	1.000	4.370	8.496	12.17	14.09	16.59	20.35
283.15	1.135	4.906	9.456	13.44	15.50	18.18	22.16
288.15	1.271	5.457	10.41	14.71	16.96	19.77	23.85

Table AI. Continued

T (K)	κ(S-m^{-1})						
293.15	1.414	6.021	11.40	16.01	18.39	21.35	25.61
298.15	1.561	6.596	12.38	17.30	19.83	22.90	27.34
303.15	1.711	7.182	13.38	18.59	21.24	24.45	29.06
308.15	1.865	7.776	14.39	19.88	22.65	25.98	30.75
313.15	2.020	8.360	15.38	21.19	24.02	27.48	32.42
318.15	2.175	8.954	16.35	22.43	25.35	28.94	34.04
323.15	2.326	9.527	17.29	23.62	26.64	30.38	35.58
	8.051	9.747	11.53	13.37	15.13		
	(m)	(m)	(m)	(m)	(m)		
273.15	19.15	19.41	18.98	18.26	17.38		
278.15	20.97	21.23	20.78	20.03	19.11		
283.15	22.76	23.03	22.61	21.83	20.85		
288.15	24.51	24.78	24.37	23.61	22.58		
293.15	26.27	26.57	26.12	25.28	24.25		
298.15	28.01	28.31	27.85	26.99	25.94		
303.15	29.74	30.05	29.60	28.69	27.61		
308.15	31.45	31.77	31.31	30.42	29.29		
313.15	33.15	33.46	33.03	32.08	30.94		
318.15	34.79	35.11	34.66	33.73	32.57		
323.15	36.37	36.70	36.20	35.33	34.15		
	10% Methanol−water mixture						
	0.1073	0.4373	1.117	2.479	4.073	6.010	7.222
	(m)	(m)	(m)	(m)	(m)	(m)	(m)
273.15	0.6180	2.606	5.062	9.655	13.34	16.77	17.58
278.15	0.7191	3.003	5.767	10.83	14.82	18.47	19.35
283.15	0.8258	3.417	6.491	12.03	16.33	20.22	21.11
288.15	0.9340	3.845	7.241	13.24	17.81	21.95	22.84
293.15	1.047	4.286	7.987	14.48	19.33	23.64	24.59
298.15	1.165	4.738	8.762	15.68	20.83	25.31	26.31
303.15	1.287	5.207	9.550	16.92	22.35	26.99	28.02
308.15	1.410	5.670	10.33	18.17	23.81	28.63	29.72
313.15	1.536	6.137	11.10	19.33	25.24	30.23	31.36
318.15	1.663	6.600	11.87	20.51	26.66	31.76	32.95
323.15	1.792	7.054	12.63	21.70	27.98	33.28	34.48
	9.030	10.61	12.09	14.42			
	(m)	(m)	(m)	(m)			
273.15	17.84	17.61	17.73	16.35			
278.15	19.61	19.37	19.51	18.05			
283.15	21.40	21.15	21.13	19.76			
288.15	23.13	22.87	23.06	21.48			
293.15	24.85	24.57	24.75	23.14			
298.15	26.57	26.28	26.45	24.80			
303.15	28.27	27.97	27.62	26.48			
308.15	29.98	29.65	29.25	28.08			
313.15	31.62	31.30	31.30	29.71			
318.15	33.20	32.90	33.11	31.30			
323.15	34.75	34.44	34.68	32.89			

Notes. Unit: C, mol-dm^{-3}; m, mol-kg^{-1}.

Table AII. Least-Squares Fitted Values of the Parameters of the Density Equation, ($\rho = a - b(T(\mathrm{K}) - 273.15)$, for Potassium Thiocyanate in Methanol–Water Mixtures

m (mol-kg^{-1})	a (kg-m^{-3})	b (kg-m^{-3}-K^{-1})	Standard deviation in ρ
	5% Methanol-water mixture		
0.1239	1011.2 ± 0.4	0.4763 ± 0.0106	0.2
0.9961	1050.6 ± 0.3	0.5257 ± 0.0081	0.1
1.976	1087.3 ± 0.9	0.5646 ± 0.0212	0.4
2.488	1103.0 ± 0.3	0.5514 ± 0.0068	0.1
2.956	1121.8 ± 0.4	0.6282 ± 0.0088	0.2
3.547	1140.1 ± 0.4	0.6277 ± 0.0088	0.2
3.931	1152.5 ± 0.4	0.6483 ± 0.0087	0.2
4.112	1147.1 ± 0.3	0.6535 ± 0.0077	0.1
4.468	1166.7 ± 0.4	0.6367 ± 0.0109	0.2
4.972	1180.7 ± 0.4	0.6540 ± 0.0096	0.2
5.490	1195.0 ± 0.4	0.6827 ± 0.0088	0.2
5.943	1206.7 ± 0.5	0.6785 ± 0.0125	0.2
7.082	1232.5 ± 0.5	0.6915 ± 0.0124	0.2
8.007	1253.8 ± 0.4	0.7078 ± 0.0098	0.2
9.114	1274.7 ± 0.5	0.7329 ± 0.0131	0.2
9.645	1283.9 ± 0.5	0.7133 ± 0.0131	0.2
10.75	1298.1 ± 0.3	0.6707 ± 0.0070	0.1
12.17	1322.8 ± 0.5	0.6921 ± 0.0122	0.2
14.31	1350.8 ± 0.5	0.6911 ± 0.0129	0.2
	10% Methanol-water mixture		
0.2411	1005.3 ± 0.3	0.4370 ± 0.0078	0.1
0.5196	1016.8 ± 0.2	0.4455 ± 0.0056	0.1
1.016	1038.3 ± 0.3	0.4949 ± 0.0066	0.1
1.484	1057.2 ± 0.2	0.5150 ± 0.0058	0.1
2.032	1080.9 ± 0.4	0.5975 ± 0.0088	0.1
2.477	1096.0 ± 0.2	0.5650 ± 0.0051	0.1
2.967	1112.4 ± 0.4	0.6014 ± 0.0087	0.2
2.983	1111.0 ± 0.2	0.5829 ± 0.0052	0.1
3.488	1129.6 ± 0.5	0.6125 ± 0.0136	0.3
3.995	1144.4 ± 0.5	0.6255 ± 0.0117	0.2
4.986	1174.1 ± 0.6	0.6395 ± 0.0148	0.2
5.031	1174.2 ± 0.4	0.6881 ± 0.0094	0.1
5.999	1198.8 ± 0.4	0.6910 ± 0.0096	0.2
6.784	1218.8 ± 0.6	0.7086 ± 0.0138	0.2
8.108	1245.1 ± 0.3	0.6677 ± 0.0067	0.1
8.501	1255.3 ± 0.7	0.7135 ± 0.0172	0.3
10.16	1283.5 ± 0.6	0.6880 ± 0.0151	0.3
13.86	1337.9 ± 0.6	0.6856 ± 0.0145	0.3

Table AIII. Speed of Sound as Functions of Concentration and Temperature for Potassium Thiocyanate in Methanol–Water Mixtures

T (K)	u (m-s^{-1})						
	5% Methanol–water mixture						
	0.1239	0.9961	1.976	2.488	2.956	3.547	3.931
	(m)	(m)	(m)	(m)	(m)	(m)	(m)
273.15	1453.8	1495.7	1536.9	1560.1	1578.4	1600.7	1616.7
278.15	1472.0	1509.9	1547.3	1570.4	1587.1	1607.6	1621.8
283.15	1486.4	1521.9	1558.2	1578.2	1593.7	1613.5	1627.4
288.15	1500.7	1532.1	1566.2	1584.9	1599.8	1618.4	1631.0
293.15	1512.3	1541.6	1574.0	1589.7	1605.1	1622.8	1634.3
298.15	1520.6	1550.5	1578.8	1593.9	1608.9	1626.0	1636.5
303.15	1529.6	1557.7	1583.6	1597.5	1611.5	1627.6	1638.8
308.15	1537.4	1562.4	1589.1	1600.9	1613.8	1629.8	1639.4
313.15	1544.8	1566.8	1592.1	1603.1	1615.6	1630.6	1639.4
318.15	1548.5	1571.0	1593.5	1603.8	1615.9	1628.2	1639.3
323.15	1553.1	1572.0	1591.6	1604.9	1616.1	1627.8	1640.1
	4.112	4.468	4.972	5.490	5.943	7.082	8.007
	(m)	(m)	(m)	(m)	(m)	(m)	(m)
273.15	1620.7	1635.3	1652.1	1667.2	1680.4	1712.7	1737.6
278.15	1625.8	1639.3	1655.3	1670.1	1682.8	1713.5	1739.2
283.15	1632.6	1643.7	1660.1	1673.2	1686.0	1714.7	1738.4
288.15	1636.1	1647.7	1661.3	1674.3	1687.6	1714.6	1739.2
293.15	1639.1	1649.0	1663.1	1675.9	1687.1	1714.9	1736.0
298.15	1639.9	1651.4	1664.9	1676.5	1687.4	1713.6	1736.3
303.15	1641.5	1652.5	1665.3	1676.5	1688.1	1711.7	1732.8
308.15	1642.3	1652.7	1665.3	1675.6	1686.8	1709.3	1729.9
313.15	1642.1	1651.9	1663.7	1673.6	1685.0	1707.9	1726.9
318.15	1641.3	1650.6	1663.3	1672.4	1682.6	1706.1	1725.0
323.15	1639.3	1649.7	1662.6	1670.0	1681.6	1701.9	1721.8
	9.114	9.645	10.75	12.17	14.31		
	(m)	(m)	(m)	(m)	(m)		
273.15	1760.6	1769.6	1786.5	1814.7	1843.0		
278.15	1760.5	1769.3	1792.1	1812.4	1841.0		
283.15	1760.8	1769.3	1787.6	1809.7	1838.6		
288.15	1760.1	1667.0	1783.8	1806.5	1835.9		
293.15	1757.7	1765.1	1781.4	1803.0	1831.9		
298.15	1755.7	1763.7	1779.0	1796.8	1828.1		
303.15	1753.3	1760.5	1775.5	1795.3	1823.5		
308.15	1750.1	1757.6	1771.3	1792.9	1819.9		
313.15	1745.6	1753.6	1767.3	1792.1	1815.8		
318.15	1743.0	1750.1	1763.5	1786.8	1808.6		
323.15	1737.1	1745.6	1759.3	1780.9	1803.5		
	10% Methanol−water mixture						
	0.2411	0.5196	1.016	1.484	2.032	2.477	2.967
	(m)	(m)	(m)	(m)	m)	(m)	(m)
273.15	1495.5	1505.4	1521.0	1538.5	1560.4	1574.0	1591.5
278.15	1507.8	1515.8	1531.3	1547.5	1568.9	1582.0	1597.4

Table AIII. Continued

T (K)	u (m-s^{-1})						
283.15	1519.2	1525.2	1540.5	1555.0	1575.2	1586.2	1602.7
288.15	1528.0	1533.6	1548.3	1562.7	1580.0	1590.4	1605.9
293.15	1536.0	1541.0	1554.7	1567.6	1584.1	1594.6	1608.6
298.15	1543.0	1546.7	1561.6	1572.4	1588.9	1599.1	1611.3
303.15	1548.5	1551.5	1564.4	1576.4	1590.0	1599.8	1613.2
308.15	1552.8	1555.3	1567.8	1579.5	1591.5	1601.4	1613.4
313.15	1556.0	1558.5	1569.9	1578.5	1592.9	1601.8	1613.5
318.15	1558.0	1560.9	1571.5	1581.6	1593.7	1601.4	1611.5
323.15	1558.8	1561.7	1571.5	1582.7	1592.9	1599.6	1610.8
	2.983	3.488	3.995	4.986	5.031	5.999	6.784
	(m)	(m)	(m)	(m)	(m)	(m)	(m)
273.15	1591.5	1608.9	1624.6	1659.6	1657.0	1682.8	1705.6
278.15	1597.5	1613.2	1628.7	1663.4	1659.0	1685.2	1704.5
283.15	1602.0	1616.9	1631.6	1664.7	1659.6	1684.7	1706.0
288.15	1605.5	1621.7	1634.2	1665.6	1660.6	1685.0	1702.9
293.15	1608.9	1623.1	1635.4	1663.2	1659.6	1684.2	1703.5
298.15	1611.1	1624.4	1636.6	1664.3	1662.2	1683.4	1702.4
303.15	1612.4	1625.7	1636.7	1660.0	1659.8	1682.1	1699.7
308.15	1612.7	1624.9	1637.0	1660.6	1658.0	1679.7	1698.3
313.15	1612.9	1624.1	1637.2	1658.5	1656.2	1677.2	1707.1
318.15	1611.9	1622.8	1633.7	1658.9	1654.2	1674.0	1692.3
323.15	1610.5	1620.4	1632.1	1651.5	1650.4	1670.4	1687.4
	8.108	8.501	10.16	13.86			
	(m)	(m)	(m)	(m)			
273.15	1735.7	1744.3	1774.7	1831.3			
278.15	1733.3	1744.1	1772.9	1829.2			
283.15	1733.9		1771.0	1825.1			
288.15	1732.9	1736.7	1767.5	1820.4			
293.15	1731.9	1730.9	1764.8	1818.2			
298.15	1728.0	1729.1	1761.4	1812.7			
303.15	1725.4	1731.2	1757.3	1807.6			
308.15	1721.5	1727.8	1754.2	1803.5			
313.15	1718.8	1724.6	1749.3	1798.5			
318.15	1712.9	1720.3	1744.0	1792.9			
323.15	1710.5	1715.9	1740.3	1787.8			

Table AIV. Viscosity of Potassium Thiocyanate in Methanol−Water Mixtures as Functions of Salt Concentration and Temperature

T (K)	η (mPa-s)						
	5% Methanol–water mixture						
	0.1239	0.9961	1.589	2.524	2.956	3.184	3.931
	(m)	(m)	(m)	(m)	(m)	(m)	(m)
273.15	2.102	1.911	1.826	1.762	1.730	1.737	1.717
278.15	1.784	1.645	1.580	1.537	1.516	1.523	1.526

Table AIV. Continued

T (K)	η (mPa-s)						
283.15	1.546	1.429	1.379	1.354	1.345	1.344	1.353
288.15	1.314	1.250	1.214	1.205	1.192	1.199	1.215
293.15	1.176	1.113	1.081	1.077	1.074	1.078	1.105
298.15	1.049	0.9942	0.9690	0.9729	0.9716	0.9764	1.013
303.15	0.9129	0.8862	0.8758	0.8836	0.8854	0.8901	0.9164
308.15	0.8076	0.7958	0.7950	0.8069	0.8102	0.8156	0.8434
313.15	0.7184	0.7168	0.7278	0.7422	0.7451	0.7504	0.7781
318.15	0.6451	0.6563	0.6685	0.6846	0.6887	0.6947	0.7249
323.15	0.5891	0.6012	0.6158	0.6345	0.6401	0.6464	0.6747
	4.112	4.183	4.468	4.972	5.490	6.382	7.082
	(m)	(m)	(m)	(m)	(m)	(m)	(m)
273.15	1.730		1.747	1.776	1.810	1.885	1.945
278.15	1.525		1.544	1.571	1.604	1.673	1.726
283.15	1.360		1.377	1.402	1.433	1.493	1.549
288.15	1.219	1.243	1.239	1.261	1.289	1.347	1.399
293.15	1.101	1.122	1.121	1.135	1.169	1.226	1.270
298.15	1.001	1.019	1.020	1.039	1.067	1.120	1.163
303.15	0.9148	0.9322	0.9330	0.9515	0.9775	1.028	1.067
308.15	0.8419	0.8548	0.8594	0.8775	0.8995	0.9483	0.9835
313.15	0.7776	0.7901	0.7940	0.8124	0.8339	0.8793	0.9151
318.15	0.7220	0.7333	0.7375	0.7547	0.7757	0.8185	0.8548
323.15	0.6741	0.6827	0.6869	0.7045	0.7248	0.7649	0.7992
	8.007	9.114	9.645	10.75	12.17	14.31	
	(m)	(m)	(m)	(m)	(m)	(m)	
273.15	2.048	2.176	2.272	2.426	2.612	3.113	
278.15	1.823	1.940	2.025	2.163	2.324	2.766	
283.15	1.639	1.743	1.819	1.945	2.090	2.482	
288.15	1.481	1.576	1.646	1.761	1.895	2.238	
293.15	1.348	1.436	1.516	1.603	1.728	2.032	
298.15	1.234	1.315	1.374	1.466	1.580	1.861	
303.15	1.138	1.211	1.266	1.350	1.456	1.711	
308.15	1.053	1.123	1.171	1.249	1.348	1.581	
313.15	0.9768	1.042	1.088	1.162	1.266	1.460	
318.15	0.9121	0.9726	1.017	1.084	1.168	1.361	
323.15	0.8573	0.9114	0.9520	1.015	1.093	1.277	
	10% Methanol–water mixture						
	0.2411	0.5196	1.016	1.484	2.032	2.477	2.967
	(m)	(m)	(m)	(m)	(m)	(m)	(m)
273.15	2.431	2.306	2.163	2.054	1.987	1.950	1.892
278.15	2.022	1.939	1.837	1.759	1.715	1.693	1.648
283.15	1.711	1.652	1.581	1.525	1.495	1.480	1.453
288.15	1.470	1.428	1.378	1.336	1.317	1.310	1.291
293.15	1.278	1.249	1.212	1.182	1.170	1.168	1.156
298.15	1.122	1.102	1.077	1.056	1.048	1.050	1.044
303.15	0.9945	0.9899	0.9632	0.9493	0.9466	0.9498	0.9476
308.15	0.8863	0.8891	0.8685	0.8584	0.8596	0.8638	0.8648

Table AIV. Continued

T (K)	η (mPa-s)						
313.15	0.7974	0.8036	0.7880	0.7814	0.7838	0.7906	0.7949
318.15	0.7226	0.7227	0.7193	0.7156	0.7189	0.7271	0.7341
323.15	0.6584	0.6588	0.6597	0.6586	0.6653	0.6719	0.6838
	2.983	3.488	3.995	4.986	5.031	5.999	7.222
	(m)	(m)	(m)	(m)	(m)	(m)	(m)
273.15	1.929	1.932	1.889	1.959	1.952	2.055	2.156
278.15	1.674	1.681	1.657	1.725	1.726	1.814	1.901
283.15	1.472	1.490	1.467	1.532	1.533	1.621	1.695
288.15	1.307	1.315	1.316	1.369	1.373	1.441	1.521
293.15	1.170	1.180	1.182	1.234	1.239	1.302	1.377
298.15	1.055	1.067	1.071	1.122	1.127	1.185	1.256
303.15	0.9567	0.9707	0.9830	1.016	1.029	1.086	1.153
308.15	0.8732	0.8865	0.9007	0.9392	0.9488	1.002	1.060
313.15	0.8023	0.8168	0.8285	0.8649	0.8769	0.9212	0.9808
318.15	0.7413	0.7563	0.7667	0.8012	0.8137	0.8525	0.9118
323.15	0.6871	0.7009	0.7127	0.7463	0.7470	0.7982	0.8512
	8.501	10.16	12.09	13.86			
	(m)	(m)	(m)	(m)			
273.15	2.321	2.519	2.974	3.292			
278.15	2.062	2.234	2.626	2.916			
283.15	1.839	2.003	2.343	2.600			
288.15	1.657	1.800	2.104	2.345			
293.15	1.502	1.658	1.919	2.124			
298.15	1.355	1.547	1.739	1.937			
303.15	1.243	1.379	1.583	1.775			
308.15	1.148	1.266	1.461	1.637			
313.15	1.065	1.207	1.354	1.515			
318.15	0.9926	1.109	1.259	1.409			
323.15	0.9283	1.027	1.170	1.315			